

## RESEARCH ARTICLE

# Remote Excitation of Neuronal Circuits Using Low-Intensity, Low-Frequency Ultrasound

William J. Tyler<sup>1,2\*</sup>, Yusuf Tufail<sup>1</sup>, Michael Finsterwald<sup>3</sup>, Monica L. Tauchmann<sup>1</sup>, Emily J. Olson<sup>1</sup>

**1** School of Life Sciences, Arizona State University, Tempe, Arizona, United States of America, **2** Hasso Plattner Institute for Bioengineering, Arizona State University, Tempe, Arizona, United States of America, **3** Array Therapeutics, Inc., San Diego, California, United States of America

## Abstract

Possessing the ability to noninvasively elicit brain circuit activity yields immense experimental and therapeutic potential. Current employed neurostimulation methods rely on the somewhat invasive use of stimulating electrodes or magnetic fields. However, the ability to noninvasively propagate through bone and other tissues in a focused manner, the implementation of low-intensity, low-frequency ultrasound (LILFU) provides a compelling alternative approach to current neuromodulation strategies. Here, we investigated the effects of LILFU on neuronal activity. By transmitting US waveforms through hippocampal slices, we determined LILFU is capable of remotely and noninvasively exciting neurons and network activity. LILFU can stimulate electrical activity in neurons by activating voltage-gated sodium channels, as well as calcium signaling. The LILFU-induced changes in neuronal activity were sufficient to trigger SNARE-mediated exocytosis in hippocampal circuits. Because LILFU can stimulate electrical activity and calcium signaling in neurons, we conclude US provides a powerful tool for remotely modulating brain circuit activity.

**Citation:** Tyler WJ, Tufail Y, Finsterwald M, Tauchmann ML, Olson EJ, et al. (2008) Remote Excitation of Neuronal Circuits Using Low-Intensity, Low-Frequency Ultrasound. PLoS ONE 3(10): e3511. doi:10.1371/journal.pone.0003511

**Editor:** Hiromu Tanimoto, Max-Planck-Institut fuer Neurobiologie, Germany

**Received:** May 6, 2008; **Accepted:** October 3, 2008; **Published:** October 29, 2008

**Copyright:** © 2008 Tyler et al. This is an open-access article distributed under the terms of the Creative Commons Attribution License, which permits unrestricted use, distribution, and reproduction in any medium, provided the original author and source are credited.

**Funding:** Studies were supported by start-up funds provided by Arizona State University. The funders had no role in study design, data collection and analysis, decision to publish, or preparation of the manuscript.

**Competing interests:** The authors have declared that no competing interests exist.

\* E-mail: wtyler@asu.edu

## Introduction

Neuromodulation techniques such as deep brain stimulation (DBS) and repetitive transcranial magn-

widespread attention due to their therapeutic utility in managing numerous neurological/psychiatric control has recently made significant advances by demonstrations of millisecond optical control of intact brain circuits [2]. Ultrasound (US) as a means of exciting [3] and reversibly suppressing [4] is effective on a gross level several decades ago. Since then however, explorations into the use of US are relatively sparse. The focus has instead been on employing more traditional approaches such as pharmacological and photonic stimulation of neuronal circuits.

Coupling its ability to interact with biological tissues [5] and its noninvasive transmission through skin in a focused manner [6]–[8], US holds promise as a potentially powerful neurostimulation tool [9], replacing currently invasive DBS strategies. Ultrasound can produce bioeffects by acting through the mechanisms as it propagates through tissues in pulsed or continuous waveforms [5], [11]–[13]. This is characterized as low-power/low-intensity or high-power/high-intensity [5]. High-intensity focused ultrasound ablation of tissue implements peak power levels often exceeding  $1000 \text{ W/cm}^2$ , whereas non-thermal effects are well described at power levels ranging from  $30\text{--}500 \text{ mW/cm}^2$  [5], [11]–[13].

Modulation of ionic conductance produced by adiabatic processes as US propagates rapidly and transiently may alter the activity of individual neurons due to the elastic nature of lipid bilayers and the spring-like transmembrane protein channels. In partial support of this hypothesis, low-power US has been shown to modulate the conductance of frog skin epidermis [12]. In addition, US exposure can induce a reversible increase in calcium influx in fibroblasts [14]. In rat thymocytes, stimulation with US can modulate  $\text{K}^+$  influx and efflux [15]. Ion channels, as well as neurotransmitter receptors possess mechanosensitive properties that render them susceptible to transient changes in lipid bilayer tension [16], [17]. Whether or not ion channels can be modulated by US is unknown. Several investigations have demonstrated however that US modulates neuronal activity by changing amplitudes and/or conduction velocities of evoked nerve potentials [3], [4], [18]–[24].

In a pioneering study, Fry and colleagues (1950) first demonstrated US is capable of modulating neuronal activity. Following temporary suppression of spontaneous activity following US transmission through crayfish ventral nerve, Fry and colleagues (1958) demonstrated that high-intensity light-evoked potentials recorded in the visual cortex [4]. Rinaldi and colleagues (1991) demonstrate that US modulates hippocampal slices with  $0.75 \text{ MHz}$  US (temporal average intensity;  $I_{\text{TA}} \sim 80 \text{ W/cm}^2$ ), significantly reducing action potentials in CA1 pyramidal neurons. In the dentate gyrus of hippocampal slices, focused US pulses can excite and suppress electrically evoked field potentials [21]. In cat saphenous nerve bundles it has been demonstrated that US is capable of differentially effecting A $\delta$ - and C-fibers depending on the intensity and duration of US irradiation of nerve bundles. Tsui and colleagues (2005) reported that a temporal average intensity of  $1 \text{ W/cm}^2$  continuously increased the amplitude of compound action potentials (CAP), while both  $2$  and  $3 \text{ W/cm}^2$  intensities decreased CAP amplitude. Rinaldi and colleagues (1990) also reported differential excitatory and inhibitory effects of US on frog sciatic nerve. In the cat auditory nerve has been achieved *in vivo* using  $5\text{-MHz}$  US pulses ( $68 \mu\text{sec}$ ;  $\sim 30 \text{ W/cm}^2$ ) [22]. US pulses have been shown to activate deep nerve structures in the hand by differentially producing tactile allodynia [3].

Although numerous intriguing studies examining the influence of US on neuronal activity have been investigations have implemented high-intensity US, which can destroy nervous tissue. Thus, we dec low-intensity ultrasound on neuronal activity. Most of the prior investigations examining the effect o high-frequency US ( $>1$  MHz; for exceptions see [3], [20], [21]), which has larger attenuation coeffi ultrasound. Medical diagnostic US typically operates from 1 to 15 MHz while therapeutic US is usuall frequencies around 1 MHz [11]. We chose to pursue our investigations here using low-frequency US mathematical models and experimental data indicate the optimal gain between transcranial transmi  $\sim 0.60$ – $0.70$  MHz [25], [26]. Detailed cellular investigations into the influence of US on neuronal act underlying US modulation of neuronal activity remain unknown. By optically monitoring changes in i neurons and synaptic transmission from individual release sites we investigated the influence of low (LILFU) on central nervous system activity.

## Results

### LILFU activates voltage-gated sodium channels in neurons

We transmitted LILFU waveforms through hippocampal slice cultures from remotely positioned tissu transducers (Figure 1A). We constructed LILFU waveforms by repeating US tone bursts at variable  $\mu$  1B). Measured using a needle hydrophone a points in the recording chamber, which corresponded to predominant LILFU waveform used in our studies (LILFU-1) had a pulse average intensity ( $I_{PA}$ ) of 2. intensity ( $I_{TA}$ ) of  $23 \text{ mW/cm}^2$ . Figure 1C illustrates a typical pressure wave obtained for a single US LILFU-1.



**Figure 1. Generation and propagation of LILFU waveforms through neuronal**

(A) General experimental configuration implemented to transmit LILFU waveforms thr monitoring neuronal activity. (B) Graphical illustration of some of the variables involved in constru variables include acoustic frequency ( $f$ ), the number of acoustic cycles per tone burst ( $c/tb$ ), tone l repetition frequency (PRF), and number of tone bursts per stimulus ( $Ntb$ ). (C) Acoustic pressure w tone burst consisting of 10 acoustic cycles at  $f = 0.44$  MHz and FFT of this US tone burst (*right*). F US stimulus waveform (LILFU-1), we used a linearly sweeping PRF by repeating the illustrated ton period.

doi:10.1371/journal.pone.0003511.g001

By imaging organotypic hippocampal slice cultures bath-loaded with the  $\text{Na}^+$  indicator CoroNa Greer  $\text{Na}^+$  transients in hippocampal CA1 pyramidal neurons ( $\Delta F/F_0 = 0.05 \pm 0.006$ ,  $n = 24$ , 6 slices; Figur  $\text{Na}^+$  channel pore blocker tetrodotoxin (TTX;  $1 \mu\text{M}$ ), blocked  $\text{Na}^+$  transients evoked by LILFU-1 (Fig that LILFU-1 increased the  $\text{Na}^+$  conductance in hippocampal neurons by stimulating the opening of , aimed to determine if LILFU waveforms were also capable of triggering action potentials in CA1 pyr single action potentials in response to the delivery of individual LILFU tone bursts during whole-cell pyramidal neurons ( $n = 4$ , 4 slices; Figure 2B). We determined however, whole-cell electrophysiolog



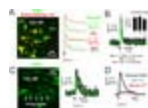


**Figure 3. LILFU triggers voltage-dependent somatic and presynaptic  $\text{Ca}^{2+}$  transients.**

(A) Confocal image (*left*) of a slice culture loaded with OGB-1 AM (*green*) to monitor  $\text{Ca}^{2+}$  transients and 101 (*red*) to identify glial cells (*yellow*). Representative LILFU-triggered  $\text{Ca}^{2+}$  transients and glial cells are illustrated (*right*). (B) Individual (*black*) and averaged (*green*)  $\text{Ca}^{2+}$  transients in response to a brief LILFU waveform. The histogram (*inset*) illustrates trial 1 normalized mean  $\text{Ca}^{2+}$  transients of repeated trials of LILFU stimulation ( $n = 19$  cells from 3 slices). (C) Confocal image (*left*) of a slice illustrating *en passant* boutons located in CA1 SR. Individual (*black*) and averaged (*green*) presynaptic transients produced by stimulation with LILFU-1. (D) Averaged somatic  $\text{Ca}^{2+}$  transients obtained from neurons in the presence of either TTX ( $n = 36$  from 4 slices) or  $\text{Cd}^{2+}$  ( $n = 30$  from 4 slices) in response to stimulation with LILFU-1.

doi:10.1371/journal.pone.0003511.g003

We were able to observe  $\text{Ca}^{2+}$  transients in response to pulsed US even when transducers were placed on the dorsal surface of the brain ( $n = 5$ ; data not shown). Similar to water and aqueous buffers, soft biological tissues (including brain) have high acoustic absorption coefficients. Therefore, we sought to determine if LILFU propagated through whole brain tissue to elicit neuronal activity. We imaged OGB-1 signals on the dorsal superficial surface of *ex vivo* brains ( $n = 5$ ) while transmitting LILFU waveforms through their ventral surfaces (Figure 4A). In these *ex vivo* brain preparations, we observed  $\text{Ca}^{2+}$  transients similar to those observed in thinner and less intact slice culture preparations in response to LILFU (Figure 4C).

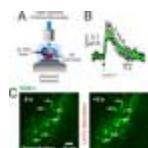


**Figure 4. LILFU waveforms transmitted through whole brains are capable of eliciting  $\text{Ca}^{2+}$  transients.**

(A) Illustration of basic experimental procedure we developed to transmit LILFU waveforms through whole brains. (B) Confocal image (*left*) of a slice culture loaded with OGB-1 AM (*green*) to monitor  $\text{Ca}^{2+}$  transients and 101 (*red*) to identify glial cells (*yellow*). Representative LILFU-triggered  $\text{Ca}^{2+}$  transients and glial cells are illustrated (*right*). (C) Individual (*black*) and averaged (*green*)  $\text{Ca}^{2+}$  transients observed in the somas of cells on the dorsal surface of the brain in response to stimulation with LILFU-1, which was transmitted through the brain from the ventral surface. (D) Confocal image (*left*) of a slice illustrating OGB-1 loaded cells on the dorsal surface of the brain. The image on *left* illustrates cells before stimulation, and the image on *right* illustrates cells two-seconds after stimulation with LILFU-1 ensued.

doi:10.1371/journal.pone.0003511.g004

### LILFU triggers SNARE-mediated synaptic vesicle exocytosis and synaptic transmission

To investigate the influence of LILFU on synaptic transmission we focused on studying a well-characterized synapse in the central nervous system, the hippocampal CA3-CA1 synapse. We transmitted LILFU waveforms through slices prepared from *thy-1-synaptophluorin* (spH) mice [33]. The pH-dependent optical probe of synaptic neurotransmitter release through an increase in fluorescence when protons are released from synaptic vesicles. Transmission of LILFU-1 through slices triggered synaptic vesicle exocytosis producing a  $\Delta F_{\text{spH}}$  of 18% ( $n = 148$  from 15 slices) in CA1 *stratum radiatum*, which primarily represent CA3-CA1 synapses (Figure 5). We identified several other LILFU waveforms, which were also effective at triggering synaptic vesicle release.

LILFU waveform composed of different US tone bursts ( $f = 0.67$  MHz, TBD = 74.5 msec, c/tb = 50, 1 Hz with Ntb = 5) also stimulated synaptic vesicle release ( $\Delta F_{\text{spH}} = 12.86 \pm 2.6\%$ ,  $n = 74$  from 6 slices). Responses obtained as a function of acoustic intensity across several different LILFU waveforms used to examine excitatory CA3-CA1 hippocampal synapses, we implemented a DiOlistic labeling approach [19]. In CA1 apical dendrites in *thy-1*-spH slices cultures. Indeed, LILFU-1 stimulated synaptic vesicle release (Figure 6).

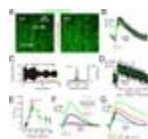


**Figure 5. LILFU stimulates SNARE-mediated synaptic vesicle exocytosis and calcium release.**

(A) Confocal images illustrating spH signals obtained before (*left*) and during (*right*) stimulation. Individual (*black*) and averaged (*green*) spH signals typically obtained in response to stimulation. (B) Acoustic pressure wave (*left*) produced by a single LILFU tone burst consisting of 50,000 cycles and FFT of LILFU tone burst (*right*). (C) Individual (*black*) and averaged (*green*) spH signals obtained in response to the LILFU tone burst shown in (C) delivered at a PRF = 10 Hz for 0.5 s to produce Np = 5. (D) Histogram of acoustic intensity. Responses from individual experiments are indicated by *black crosses* and averaged responses indicated by the *green line*. (E) Averaged spH signals illustrating the effect of CNQX+APV ( $n = 84$  slices), or BoNT/A ( $n = 60$  from 4 slices) on synaptic vesicle exocytosis induced by LILFU-1. (F) Average buttons in response to field stimulation of Schaffer collaterals with 250 AP, 50 Hz ( $n = 48$ ), 100 AP, 50 Hz ( $n = 51$ ), or by LILFU-1 ( $n = 148$ ).

doi:10.1371/journal.pone.0003511.g005



**Figure 6. Influence of LILFU on putative excitatory hippocampal CA3-CA1 synapses.**

(A) Confocal images illustrating spH expression in CA1 SR (*left*) and an apical dendrite (*right*) which was labeled with DiI using a DiOlistic labeling technique (*middle*). The two-channel confocal images show excitatory synapses indicated by apposition of spH<sup>+</sup> puncta and dendritic spines. (B) Individual (*black*) and averaged (*green*) DiI (*red*) signals obtained from terminals impinging on dendritic spines in response to stimulation with LILFU-1.

doi:10.1371/journal.pone.0003511.g006

Hyperosmotic shock produced by application of sucrose to hippocampal synapses is capable of stimulating primed synaptic vesicles (~10 vesicles) in a Ca<sup>2+</sup>-independent manner and is thought to occur from the nature of mechanical energy conferred by acoustic waves, we questioned whether some part of the response observed in response to LILFU might be due to mechanical interactions on vesicle release machinery at active zones and synaptic vesicles. Since hypertonic sucrose application is still capable of triggering exocytosis at hippocampal synapses lacking the SNARE-protein SNAP-25 [37], we aimed to determine if LILFU-1 could stimulate neurotransmitter release after cleaving SNAP-25 by treating slice cultures with botulinum neurotoxin A (BoNT/A). Indicating that pulsed US-induced exocytosis is SNARE-mediated and not likely due to mechanisms such as hyperosmotic shock, treatment of slice cultures with BoNT/A nearly abolished spH responses produced by LILFU (Figure 5F).



Addition of TTX almost completely blocked vesicular release in response to LILFU-1 highlighting the action potentials in LILFU-triggered synaptic vesicle release (Figure 5F). Blocking excitatory network (100  $\mu$ M) reduced the  $\Delta F_{\text{spH}}$  by  $\sim 50\%$  compared to controls indicating that LILFU stimulates synaptic activity not merely exocytosis (Figure 5F). Interestingly, the kinetics and amplitudes of LILFU-triggered spH obtained in response to electrical stimulation of CA3 Schaffer collaterals using monopolar electrodes responses previously reported [33], [38]. Since spH typically produces a  $\Delta F$  of  $\sim 1\text{--}2\%$  per released vesicle, LILFU-1 to stimulate the release of  $\sim 15$  vesicles per release site.

## Discussion

In this study we tested whether LILFU was capable of directly stimulating the activity of neurons in several novel observations in our study. From a mechanistic view, we observed that US stimulates neurons by triggering voltage-gated  $\text{Na}^+$  transients and voltage-dependent  $\text{Ca}^{2+}$  transients. We further observed that these activity were sufficient to trigger SNARE-mediated synaptic vesicle exocytosis and synaptic transmission driving network activity.

The mechanisms underlying US activation of voltage-sensitive channels in neurons are presently unknown. The mechanical nature of US and its interactions with neuronal membranes leads to the opening of mechanosensitive channels. Supporting this hypothesis, we observed that TTX a voltage-gated  $\text{Na}^+$  channel pore-blocker blocked  $\text{Na}^+$  transients. Further, many voltage-gated  $\text{Na}^+$  channels (i.e. NaV 1.2, 1.4, 1.5, and 1.6) are known to have mechanical sensitivity [16], [17]. The addition of TTX also blocked a large portion of LILFU-induced activity. The action of LILFU may be on voltage-gated  $\text{Na}^+$  channels. However, the addition of  $\text{Cd}^{2+}$  further reduced activity which suggests at least some voltage-gated  $\text{Ca}^{2+}$  channels may be sensitive to LILFU. Indeed, L-type  $\text{Ca}^{2+}$  channels have been shown to be mechanically sensitive under various conditions [16], [17].

Further studies are required to identify which ion channels are sensitive to US, as well as to characterize US as a function of acoustic intensity. By imaging large fields of view and monitoring the responses observed that LILFU-1 stimulated activity in  $\sim 30\%$  of the neurons in a given field. These observations raise the question for instance whether neurons, which have been recently active, are less susceptible to US stimulation. The kinetic states of a neuron's ion channels may shape how responsive a given cell is to US stimulation. We are currently in the process of investigating the individual properties of US waveforms (peak and temporal average intensity, tone burst/pulse duration) which will also likely determine how effective a given waveform is at stimulating neuronal activity. With regard to waveform, we observed that US waveforms having moderate intensities were more robust in triggering neuronal activity than US waveforms possessing lower or higher intensities. Future studies investigating the influence of US waveform parameters such as tone-burst duration (pulse length), pulse repetition frequency, and acoustic intensity. Understanding how waveform characteristics contribute to the action of US is an important issue to resolve. One particularly interesting question is can LILFU be used in a molecular biology application inducing protein specific resonances using an optimal acoustic frequency or particular LILFU waveform.

## Potential biohazardous effects of US

Having a long and proven safety record, US is widely used for diagnostic medical imaging, as well as [13]. Ultrasound is however quite capable of destroying biological tissues, so when employing US to potential for biohazardous effects must be carefully considered. Many of the hazards associated with large thermal fluctuations and/or cavitation damage in soft tissues. Although many groups have p US on neuronal activity [3], [4], [18]–[24], these results are unique in that we found US is capable lower acoustic intensities than those previously reported. Some groups have utilized acoustic intens neuronal activity in hippocampal brain slices [19], whereas other groups have used intensities exce peripheral pain sensations in humans [3]. In this study we implemented a range of acoustic intensit US have been well documented in other tissues (30–500 mW/cm<sup>2</sup>) [5], [11]–[13]. Further, the US i stimulating neuronal activity are below the output power limits set by the United States Food and D imaging.

Due to the lack of gas bodies in most soft tissues including brain [13], we do not expect cavitation t using LILFU to stimulate brain activity *in vivo*. In most soft tissues, cavitation rarely induces damage lung, intestinal, and cardiac tissues in which cavitation damage can occur at pressures ~2 MPa du occurring gas bodies) [13]. The peak rarefactional pressure used in our studies was <1 MPa. At the cavitation damage was not induced in hippocampal slice cultures. Besides the potential biohazards tissue, the possibility for damage arising from repeated, long-term US exposure needs to be evaluat effects of chronic US administration on brain function. We found that chronic LILFU stimulation (36– of neuronal membranes. Demonstrating the need for caution however, a recent study reported that producing some disruption of neuronal migration in the cortex of developing mouse embryos [40].

### **The effects of US on molecular signal transduction pathways**

While we have studied the actions of US on neuronal activity by monitoring ionic conductance and s recognize US may influence signaling molecules capable of influencing neuronal function. In other ti molecules also present in neuronal tissues are known to be influenced by US. For example, low-inte signaling, which triggers the differentiation of human mesenchymal stem cells into chondrocytes [4: been shown to stimulate the production of bFGF, TGF- $\beta$ , BMP-7, VEGF, and IGF-1 [42]–[45]. Certain IGF-1 have differential yet significant effects on the nervous system by affecting processes involved growth/survival [46], [47], cell fate specification, tissue patterning, axon guidance in the nervous sy brain [49]. Moreover, VEGF [49], [50], TGF- $\beta$  [51], [52], and bFGF [46] are neuroprotective against neurodegeneration. These observations prompt the intriguing question of whether it is possible for l brain or the production and secretion of growth factors such as brain-derived neurotrophic factor, n

Additional actions on conserved cell signaling pathways further support explorations into the use of is known to regulate neuronal survival and plasticity [53]. Integrin-linked kinase (ILK) and Akt are k establishing neuronal polarity [54]. The PI3K-Akt signaling pathway is capable of blocking cell death neuronal cell types [55]. Ultrasound induces cyclooxygenase-2 expression in human chondrocytes b  $\kappa$ B/ and p300 signaling pathway [56], while in murine osteoblasts US stimulates COX-2 expression , ERK signaling pathway [57]. It should be determined if US is also capable of stimulating ILK, PI3K, ,



neurons as these signaling molecules may become important targets for future ultrasonic neuromod

## Feasibility of delivering LILFU to intact nervous systems and brains for neuromodulation

As a tool for modulating neuronal function, US has been studied and considered across a range of u tissues to its ability to produce sensory perceptions [6], [9], [10]. Gavrilov and colleagues (1976) w capable of activating both superficial and deep peripheral nerve structures in humans, which lead to sensations. In these studies however, US was only transmitted through soft tissues such as the skin Whether US will be effective in the noninvasive transcranial regulation of neuronal circuits in the int determined.

Transcranial ultrasonography of the basilar artery has been shown to trigger auditory sensations in have reported similar observations in animals during delivery of transcranial US and at least one un involve the direct stimulation of auditory nerve fibers by US [10]. Collectively, these observations d of evoking sensory stimuli even in humans. Despite these exciting observations, the skull is a major transmission of US into intact brains for neurostimulation purposes. The skull reflects, refracts, abs impedance mismatches between the skin, skull, and skull-brain interfaces also present a challenge f into the intact brain. The frequency of US we chose for the construction of LILFU waveforms (0.44–( optimal gains have been previously reported between transcranial US transmission and brain absorp transmission and attenuation coefficients, as well as experimental data examining the transmission the optimal gain for the transcranial US transmission and brain absorption is between 0.60 and 0.7( observations and the findings of others, it is likely that LILFU fields can be transmitted through skull neurostimulation purposes similar to methods using rTMS. In order to achieve targeted neurostimul focus LILFU fields.

It is possible to focus US fields using a variety of approaches. Pulsed US (<1 MHz) can be focused tl 1 mm of intended loci using phased US transducer arrays [6], [8], [59]. Based on observations rep investigate US field focusing through human skulls [6], [8], [59], US may be able to confer a spatia by currently implemented neuromodulation strategies such as vagal nerve stimulation and DBS, wh therapeutic value [1], [60]. Before the feasibility of using focused LILFU for targeted neurostimulati determined, future studies must directly address how focused US fields influence the activity of neu

## Conclusions

Our observations demonstrate that LILFU can be used to remotely stimulate the activity of central n *vitro*. We have provided the first direct evidence that US modulates the ionic conductance of neuron activity and synaptic transmission in a manner sufficient to stimulate neuronal circuits. Several issu potential of US in controlling neuronal activity can be realized. Since US is capable of being focused one tantalizing possibility is that LILFU may permit deep-brain stimulation without the need for surg invasive procedures.

## Materials and Methods

## Preparation of slice cultures and *ex vivo* brains

All procedures involving mice were conducted in accordance with federal guidelines and protocols at the Institutional Animal Care and Use Committee at Arizona State University. Hippocampal slice cultures were prepared from YFP, or wild-type mice similar to previously described methods [61]. Briefly, transverse hippocampal slices were prepared using a wire slicer (MX-TS, Siskiyou, Inc., Grants Pass, Oregon, USA) and maintained *in vitro* on Millicell-CM inserts (Millipore, Bedford, MA) in a 36°C, 5% CO<sub>2</sub>, humidified (99%) incubator. Slices were used for experiments *in vitro*. In some experiments to cleave SNARE-proteins, BoNT/A (250 ng/mL) was added to the slice culture medium.

We prepared *ex vivo* brains using the following approach. Following CO<sub>2</sub> inhalation, wild-type mice were sacrificed and brains were removed. The dura was carefully removed and the brains were then placed in ice-cold artificial cerebrospinal fluid (aCSF) containing (in mM) 83 NaCl, 2.5 KCl, 3.3 MgSO<sub>4</sub>, 1 NaH<sub>2</sub>PO<sub>4</sub>, 26.2 NaHCO<sub>3</sub>, 22 glucose, 72 sucrose, and 0.5 CaCl<sub>2</sub>. Brains were allowed to recover for 5 min in the ice-cold aCSF before recovering for ~20 min at 36°C. *Ex vivo* brains were bulk loaded with OGB-1 AM (Invitrogen, Carlsbad, California, USA).

## Loading of slice cultures and *ex vivo* brains with fluorescent ion indicators

In order to load slice cultures prepared from wild-type mice with CoroNa Green AM (Invitrogen, Carlsbad, CA), Pluronic F-127 in DMSO (Invitrogen) was added to a 50 µg vial of CoroNa Green AM. The dye solution was added to the slice culture medium before adding 100 µL culture medium. We then added 5 µL of the dye-containing solution to 1 mL of the slice culture medium, as well as adding 5 µL to the surface of slices. Following a 10 min incubation time at 36°C, the slice culture medium, allowed to recover an additional 10 min, and then used for experiments. To load *ex vivo* brains with OGB-1 AM, we added 2 µL 20% Pluronic F-127 in DMSO and 8 µL DMSO to a 50 µg vial of OGB-1 AM. The dye-containing solution was added to the slice culture medium before adding 90 µL culture media. We next added 20 µL of this dye-containing solution to 3 mL of the slice culture medium. Slices were washed three times with slice culture medium (101 (Invitrogen; 10 µM in slice culture medium for 15 min) or allowed to recover for 30 min prior to experiments. To load *ex vivo* brains with OGB-1 AM we used a procedure similar to above, but substituted the slice culture medium with dissection aCSF. We added 60 µL of the dye-containing solution to 9 mL dissection aCSF. Brains were loaded for 30 min and washed three times and allowed to recover for an additional 30 min in dissection aCSF at room temperature.

## Confocal imaging and whole-cell patch-clamp recordings

Slice cultures or whole *ex vivo* brains were transferred to recording chambers containing recording medium containing (in mM) 83 NaCl, 2.5 KCl, 3.3 MgSO<sub>4</sub>, 10 HEPES, 10 glucose, and 2.5 CaCl<sub>2</sub>, pH 7.4 at room temperature. Recording chambers were mounted on a custom built-stage on an Olympus Fluoview FV-300 laser-scanning confocal microscope (Olympus America, Inc., Pennsylvania, USA). Excitation of spH, OGB-1 AM, and CoroNa Green AM was performed using the 488 nm line of an Ar-ion laser. In some experiments DiI was excited using a 546 nm HeNe laser. Time-series images were acquired using a 60x objective (NA) Olympus UPlanFL water-immersion lens.

Slice recording chambers consisted of culture inserts placed inside an aCSF reservoir held in place with a silicon face of the transducer. This approach produced ~4.5 mm standoff distance between the face of the transducer and the slice culture medium.

plane on the surface of slices. In a subset of experiments, slice cultures ( $n = 5$ ) were mounted near mL beaker containing immersed US transducers, which were affixed to the bottom beakers to provide image *ex vivo* brains, the ventral surface of whole *ex vivo* brains were glued to the bottom of polystyrene which were filled with aCSF and mounted above US transducers using ultrasonic coupling gel. Confo was conducted on the superficial dorsal surface of *ex vivo* brains during transmission of LILFU wave brain.

In a subset of experiments we performed whole-cell current clamp recordings from visually identified standard approaches. Briefly, patch electrode pipettes filled with an intracellular solution containing Di-Tris-P-creatine, 0.2 EGTA, 3 Mg-ATP, and 0.5 Na-GTP, 280–290 mOsm, pH 7.2; the final resistance electrodes was 5–7 M $\Omega$ . Current clamp recordings were performed using a MultiClamp 700B patch-clamp software (Molecular Devices, Sunnyvale, California, USA). Following 5–10 min of whole-cell access, recorded in response to stimulation with LILFU waveforms.

### Generation and characterization of LILFU waveforms

In our studies we used custom built PZT ultrasound transducers ( $d = 35$  mm) having a single quarter frequency of 0.53 MHz, and a  $-6$  dB fractional bandwidth of 65% with two peaks (0.44 MHz, 0.66 MHz) were generated by repeating pulse trains of US tone bursts at a pulse repetition frequency until a desired waveform had been generated (Figure 1B). Ultrasound tone bursts were generated by trains of square waves (0.2–100 kHz) using an Agilent 33220A function generator. To produce final plate voltages delivered to transducers, the signal was amplified (50 dB gain) using an ENI 240L RF amplifier. Square waves were delivered between 0.44–0.66 MHz frequency desired, while the number of square waves driving each US tone burst equaled the number of cycles in the given US tone burst. Each US tone burst (pulse) contained between 1 and 50,000 acoustic cycles desired. US tone bursts (Figure 1B) were repeated at a pulse repetition frequency by triggering the function generator with a second Agilent 33220A function generator. Pulse repetition frequencies were either 10–100 Hz or 1–10 kHz waveform. Our primary LILFU waveform (LILFU-1) had the following properties:  $f = 0.44$  MHz, TBD sweep 0–100 Hz, and  $N_{tb} = 250$ .

To characterize LILFU power levels, we recorded voltage waveforms produced by US pressure waveforms using a Kongsberg Corporation, Sunnyvale, California, USA) and an Agilent DSO6012A 100 MHz digital oscilloscope (Agilent Technologies, Santa Clara, California, USA). To confirm transducers were operating at the intended acoustic frequency, we performed traces recorded in response to US tone bursts. All pressure waves produced by LILFU waveforms were recorded at tissue positions in the actual recording chambers by positioning the hydrophone face using a xyz stage (MTS Systems, Eden Prairie, CA, USA) mounted on the vibration isolation table attached to the microscope stage (Figure S1). The recording chamber was held consistent across experiments. We measured acoustic intensities with and without the slice and found no effect of the presence of a slice on the acoustic waveform. The acoustic pressure and intensity were calculated using published equations and technical standards established by the American Institute of Ultrasound in Medicine and the National Electrical Manufacturers Association [62].

### Data analysis

Confocal images were analyzed offline using *ImageJ* (<http://rsb.info.nih.gov/ij/>) or the Olympus Flu changes in spH fluorescence as a percent change from baseline fluorescence levels. For OGB-1 and  $\Delta F/F_0$  using standard approaches where  $\Delta F = F - F_0$ . LILFU waveforms and electrophysiological analysis (*Pro* (WaveMetrics, Lake Oswego, Oregon, USA). Data shown are mean  $\pm$  S.E.M.

## Supporting Information

---

### Figure S1.

Characterization and operation of PZT transducers. Illustration of experimental setup used to operate waveforms through neuronal tissue. For measuring PZT properties, as well as the pressure waves produced by a calibrated hydrophone. To investigate the influence of LILFU on neuronal activity, we transmitted LILFU into hippocampal slice cultures while simultaneously performing confocal microscopy (see *Materials and Methods* details).

(2.80 MB TIF)

### Table S1.

(0.05 MB DOC)

### Video S1.

The video illustrates a time-lapsed series of confocal images obtained from an organotypic slice culture which was bath-loaded with OGB-1 AM. Hippocampal CA1 *stratum pyramidale* is indicated. The application of LILFU-1. As indicated by the increase in OGB-1 fluorescence intensity,  $Ca^{2+}$  transients were observed upon stimulation with LILFU-1.

(7.87 MB AVI)

### Video S2.

The video illustrates a time-lapsed series of confocal images obtained from a thy-1-spH organotypic slice culture. *stratum pyramidale* is in the upper left region of the movie with the proximal portion of *stratum radiatum* in the right quadrant of the movie. The appearance of red fluorescence indicates the delivery of LILFU-1. As indicated by the increase in fluorescence intensity, the induction of vesicle release in response to LILFU can be clearly resolved.

(7.56 MB AVI)

## Acknowledgments

---

We thank Dr. Juan Burrone, Dr. Sumon K. Pal, Dr. Catherine E. Morris, and Daaimah LaVigne for their contributions to this work.

manuscript. We also thank Dr. Andrew Trevelyan for advice on calcium-dye loading and Sam Howar technical advice hydrophone operation.

## Author Contributions

---

Conceived and designed the experiments: WJT. Performed the experiments: WJT YT MF MLT EJO. AI CM. Contributed reagents/materials/analysis tools: WJT MF. Wrote the paper: WJT YT MLT EJO.

## References

---

1. Wagner T, Valero-Cabre A, Pascual-Leone A  
(2007) Noninvasive Human Brain Stimulation. *Annu Rev Biomed Eng* 9: 527–565.
2. Zhang F, Wang LP, Brauner M, Liewald JF, Kay K, et al.  
(2007) Multimodal fast optical interrogation of neural circuitry. *Nature* 446: 633–639.
3. Gavrilov LR, Gersuni GV, Ilyinsky OB, Sirotyuk MG, Tsurulnikov EM, et al.  
(1976) The effect of focused ultrasound on the skin and deep nerve structures of man and animal. *P*
4. Fry FJ, Ades HW, Fry WJ  
(1958) Production of reversible changes in the central nervous system by ultrasound. *Science* 127: 1
5. ter Haar G  
(2007) Therapeutic applications of ultrasound. *Prog Biophys Mol Biol* 93: 111–129.
6. Hynynen K, Jolesz FA  
(1998) Demonstration of potential noninvasive ultrasound brain therapy through an intact skull. *Ultr*
7. Clement GT  
(2004) Perspectives in clinical uses of high-intensity focused ultrasound. *Ultrasonics* 42: 1087–1093
8. Clement GT, Hynynen K  
(2002) A non-invasive method for focusing ultrasound through the human skull. *Phys Med Biol* 47: 1
9. Fry WJ  
(1968) Electrical stimulation of brain localized without probes—theoretical analysis of a proposed me
10. Gavrilov LR, Tsurulnikov EM, Davies IA  
(1996) Application of focused ultrasound for the stimulation of neural structures. *Ultrasound Med Bic*
11. O'Brien WD Jr  
(2007) Ultrasound-biophysics mechanisms. *Prog Biophys Mol Biol* 93: 212–255.
12. Dinno MA, Dyson M, Young SR, Mortimer AJ, Hart J, et al.  
(1989) The significance of membrane changes in the safe and effective use of therapeutic and diagn  
1543–1552.
13. Dalecki D

- (2004) Mechanical bioeffects of ultrasound. *Annu Rev Biomed Eng* 6: 229–248.
14. Mortimer AJ, Dyson M  
(1988) The effect of therapeutic ultrasound on calcium uptake in fibroblasts. *Ultrasound Med Biol* 14
15. Chapman IV, MacNally NA, Tucker S  
(1980) Ultrasound-induced changes in rates of influx and efflux of potassium ions in rat thymocytes
16. Sukharev S, Corey DP  
(2004) Mechanosensitive channels: multiplicity of families and gating paradigms. *Sci STKE* 2004: re
17. Morris CE, Juranka PF  
(2007) *Lipid Stress at Play: Mechanosensitivity of Voltage-Gated Channels*. Academic Press. pp. 297
18. Mihran RT, Barnes FS, Wachtel H  
(1990) Temporally-specific modification of myelinated axon excitability in vitro following a single ultrasonic pulse. *Ultrasound Med Biol* 16: 297–309.
19. Tsui PH, Wang SH, Huang CC  
(2005) In vitro effects of ultrasound with different energies on the conduction properties of neural tissue. *Ultrasound Med Biol* 31: 1199–1205.
20. Rinaldi PC, Jones JP, Reines F, Price LR  
(1991) Modification by focused ultrasound pulses of electrically evoked responses from an in vitro hippocampal slice. *Brain* 114: 36–42.
21. Bachtold MR, Rinaldi PC, Jones JP, Reines F, Price LR  
(1998) Focused ultrasound modifications of neural circuit activity in a mammalian brain. *Ultrasound Med Biol* 24: 1199–1205.
22. Foster KR, Wiederhold ML  
(1978) Auditory responses in cats produced by pulsed ultrasound. *J Acoust Soc Am* 63: 1199–1205.
23. Young RR, Henneman E  
(1961) Functional effects of focused ultrasound on mammalian nerves. *Science* 134: 1521–1522.
24. Fry WJ, Wulff VJ, Tucker D, Fry FJ  
(1950) Physical factors involved in ultrasonically induced changes in living systems: I. Identification of physical factors. *Am J Phys* 22: 867–876.
25. White PJ, Clement GT, Hynynen K  
(2006) Local frequency dependence in transcranial ultrasound transmission. *Phys Med Biol* 51: 2293
26. Hayner M, Hynynen K  
(2001) Numerical analysis of ultrasonic transmission and absorption of oblique plane waves through bone. *Ultrasound Med Biol* 27: 3319–3330.
27. Meier SD, Kovalchuk Y, Rose CR  
(2006) Properties of the new fluorescent Na<sup>+</sup> indicator CoroNa Green: comparison with SBFI and CoroNa Orange. *J Biol Chem* 281: 251–259.



- Miller DL, Pislaru SV, Greenleaf JE  
(2002) Sonoporation: mechanical DNA delivery by ultrasonic cavitation. *Somat Cell Mol Genet* 27: 1
29. Feng G, Mellor RH, Bernstein M, Keller-Peck C, Nguyen QT, et al.  
(2000) Imaging neuronal subsets in transgenic mice expressing multiple spectral variants of GFP. *Neuron* 28: 103–114.
30. Trevelyan AJ, Sussillo D, Watson BO, Yuste R  
(2006) Modular propagation of epileptiform activity: evidence for an inhibitory veto in neocortex. *J Neurosci* 26: 1211–1221.
31. Paoletti P, Ascher P  
(1994) Mechanosensitivity of NMDA receptors in cultured mouse central neurons. *Neuron* 13: 645–656.
32. Maroto R, Raso A, Wood TG, Kurosky A, Martinac B, et al.  
(2005) TRPC1 forms the stretch-activated cation channel in vertebrate cells. *Nat Cell Biol* 7: 179–188.
33. Li Z, Burrone J, Tyler WJ, Hartman KN, Albeanu DF, et al.  
(2005) Synaptic vesicle recycling studied in transgenic mice expressing synaptophysin. *Proc Natl Acad Sci USA* 102: 1151–1156.
34. Miesenböck G, De Angelis DA, Rothman JE  
(1998) Visualizing secretion and synaptic transmission with pH-sensitive green fluorescence proteins. *Proc Natl Acad Sci USA* 95: 9123–9128.
35. Gan WB, Grutzendler J, Wong WT, Wong RO, Lichtman JW  
(2000) Multicolor “DiOlistic” labeling of the nervous system using lipophilic dye combinations. *Neuron* 28: 103–114.
36. Rosenmund C, Stevens CF  
(1996) Definition of the readily releasable pool of vesicles at hippocampal synapses. *Neuron* 16: 115–125.
37. Bronk P, Deak F, Wilson MC, Liu X, Sudhof TC, et al.  
(2007) Differential effects of SNAP-25 deletion on Ca<sup>2+</sup>-dependent and Ca<sup>2+</sup>-independent neurotransmission. *J Neurosci* 27: 1151–1161.
38. Sankaranarayanan S, De Angelis D, Rothman JE, Ryan TA  
(2000) The use of pHluorins for optical measurements of presynaptic activity. *Biophys J* 79: 2199–2209.
39. Burrone J, Li Z, Murthy VN  
(2006) Studying vesicle cycling in presynaptic terminals using the genetically encoded probe synaptopHluorin. *Neuron* 50: 103–114.
40. Ang ES Jr, Gluncic V, Duque A, Schafer ME, Rakic P  
(2006) Prenatal exposure to ultrasound waves impacts neuronal migration in mice. *Proc Natl Acad Sci USA* 103: 1151–1156.
41. Ebisawa K, Hata K, Okada K, Kimata K, Ueda M, et al.  
(2004) Ultrasound enhances transforming growth factor beta-mediated chondrocyte differentiation *in vitro*. *Eng* 10: 921–929.
42. Reher P, Doan N, Bradnock B, Meghji S, Harris M  
(1999) Effect of ultrasound on the production of IL-8, basic FGF and VEGF. *Cytokine* 11: 416–423.
43. Mukai S, Ito H, Nakagawa Y, Akiyama H, Miyamoto M, et al.  
(2005) Transforming growth factor-beta1 mediates the effects of low-intensity pulsed ultrasound in bone. *J Bone Miner Res* 20: 1713–1721.

- Naruse K, Miyauchi A, Itoman M, Mikuni-Takagaki Y  
(2003) Distinct anabolic response of osteoblast to low-intensity pulsed ultrasound. *J Bone Miner Res*
45. Sant'Anna EF, Leven RM, Viridi AS, Sumner DR  
(2005) Effect of low intensity pulsed ultrasound and BMP-2 on rat bone marrow stromal cell gene ex
46. Abe K, Saito H  
(2001) Effects of basic fibroblast growth factor on central nervous system functions. *Pharmacol Res*
47. Molteni R, Fumagalli F, Magnaghi V, Roceri M, Gennarelli M, et al.  
(2001) Modulation of fibroblast growth factor-2 by stress and corticosteroids: from developmental e  
*Brain Res Rev* 37: 249–258.
48. Charron F, Tessier-Lavigne M  
(2007) The Hedgehog, TGF-beta/BMP and Wnt families of morphogens in axon guidance. *Adv Exp M*
49. Gora-Kupilas K, Josko J  
(2005) The neuroprotective function of vascular endothelial growth factor (VEGF). *Folia Neuropathol*
50. Jin KL, Mao XO, Greenberg DA  
(2000) Vascular endothelial growth factor: direct neuroprotective effect in in vitro ischemia. *Proc Na*
51. Flanders KC, Ren RF, Lippa CF  
(1998) Transforming growth factor-betas in neurodegenerative disease. *Prog Neurobiol* 54: 71–85.
52. Tesseur I, Wyss-Coray T  
(2006) A role for TGF-beta signaling in neurodegeneration: evidence from genetically engineered mc
53. Mattson MP  
(2005) NF-kappaB in the survival and plasticity of neurons. *Neurochem Res* 30: 883–893.
54. Guo W, Jiang H, Gray V, Dedhar S, Rao Y  
(2007) Role of the integrin-linked kinase (ILK) in determining neuronal polarity. *Dev Biol* 306: 457–
55. Brunet A, Datta SR, Greenberg ME  
(2001) Transcription-dependent and -independent control of neuronal survival by the PI3K-Akt signa  
297–305.
56. Hsu HC, Fong YC, Chang CS, Hsu CJ, Hsu SF, et al.  
(2007) Ultrasound induces cyclooxygenase-2 expression through integrin, integrin-linked kinase, Ak  
human chondrocytes. *Cell Signal* 19: 2317–2328.
57. Tang CH, Yang RS, Huang TH, Lu DY, Chuang WJ, et al.  
(2006) Ultrasound stimulates cyclooxygenase-2 expression and increases bone formation through in  
phosphatidylinositol 3-kinase, and Akt pathway in osteoblasts. *Mol Pharmacol* 69: 2047–2057.
58. Magee TR, Davies AH  
(1993) Auditory phenomena during transcranial Doppler insonation of the basilar artery. *J Ultrasoun*

- Hynynen K, Clement GT, McDannold N, Vykhodtseva N, King R, et al.  
(2004) 500-element ultrasound phased array system for noninvasive focal surgery of the brain: a pr  
human skulls. *Magn Reson Med* 52: 100–107.
60. Andrews RJ  
(2003) Neuroprotection trek—the next generation: neuromodulation I. Techniques—deep brain stimul  
transcranial magnetic stimulation. *Ann N Y Acad Sci* 993: 1–13; discussion 48-53.
61. Stoppini L, Buchs PA, Muller D  
(1991) A simple method for organotypic cultures of nervous tissue. *J Neurosci Methods* 37: 173–182
62. NEMA  
(2004) Acoustic Output Measurement Standard for Diagnostic Ultrasound Equipment. Washington, C  
Association.

---

All site content, except where otherwise noted, is licensed under a Creative Commons Attribution License.